Received: 26 March 2019 | Revised: 13 July 2019 | Accepted: 16 July 2019

DOI: 10.1002/hbm.24737

RESEARCH ARTICLE

WILEY

Altered transient brain dynamics in multiple sclerosis: Treatment or pathology?

Jeroen Van Schependom[1,2,3] | Diego Vidaurre[4,5] | Lars Costers[1] | Martin Sjøgård[6] | Marie B. D'hooghe[1,3] | Miguel D'haeseleer[1,3] | Vincent Wens[6,7] | Xavier De Tiège[6,7] | Serge Goldman[6,7] | Mark Woolrich[4,5] | Guy Nagels[1,3,8]

[1]Center for Neurosciences, Vrije Universiteit Brussel, Brussels, Belgium

[2]Radiology, Universitair Ziekenhuis Brussel, Brussels, Belgium

[3]National MS Center Melsbroek, Melsbroek, Belgium

[4]Oxford Centre for Human Brain Activity (OHBA), University of Oxford, Oxford, UK

[5]Oxford University Centre for Functional MRI of the Brain (FMRIB), University of Oxford, Oxford, UK

[6]Laboratoire de Cartographie fonctionnelle du Cerveau, UNI-ULB Neuroscience Institute, Université libre de Bruxelles (ULB), Brussels, Belgium

[7]Magnetoencephalography Unit, Department of Functional Neuroimaging, Service of Nuclear Medicine, CUB-Hôpital Erasme, Brussels, Belgium

[8]St Edmund Hall, University of Oxford, Oxford, UK

Correspondence
Jeroen Van Schependom, Centre for Neurosciences, Vrije Universiteit Brussel, Laarbeeklaan 103, 1090 Brussels, Belgium.
Email: jeroen.van.schependom@vub.be

Funding information
Fondation Philippe Wiener - Maurice Anspach; Fonds Erasme; Belgian Charcot Foundation; Genzyme-Sanofi; Fond Erasme pour la Recherche Médicale; Fonds De La Recherche Scientifique - FNRS; Fonds Wetenschappelijk Onderzoek, Grant/Award Numbers: 11B7218N, 12I1817N, 1501218N, 1805620N

Abstract

Multiple sclerosis (MS) is a demyelinating, neuroinflammatory, and -degenerative disease that affects the brain's neurophysiological functioning through brain atrophy, a reduced conduction velocity and decreased connectivity. Currently, little is known on how MS affects the fast temporal dynamics of activation and deactivation of the different large-scale, ongoing brain networks. In this study, we investigated whether these temporal dynamics are affected in MS patients and whether these changes are induced by the pathology or by the use of benzodiazepines (BZDs), an important symptomatic treatment that aims at reducing insomnia, spasticity and anxiety and reinforces the inhibitory effect of GABA. To this aim, we employed a novel method capable of detecting these fast dynamics in 90 MS patients and 46 healthy controls. We demonstrated a less dynamic frontal default mode network in male MS patients and a reduced activation of the same network in female MS patients, regardless of BZD usage. Additionally, BZDs strongly altered the brain's dynamics by increasing the time spent in the deactivating sensorimotor network and the activating occipital network. Furthermore, BZDs induced a decreased power in the theta band and an increased power in the beta band. The latter was strongly expressed in those states without activation of the sensorimotor network. In summary, we demonstrate gender-dependent changes to the brain dynamics in the frontal DMN and strong effects from BZDs. This study is the first to characterise the effect of multiple sclerosis and BZDs in vivo in a spatially, temporally and spectrally defined way.

KEYWORDS
benzodiazepines, hidden Markov model, multiple sclerosis, transient brain dynamics

1 | INTRODUCTION

Multiple sclerosis is the most frequent cause of non-traumatic neurological disability in young and middle-age adults affecting ~2 million people worldwide (Inglese, 2006). In addition to a range of physical disabilities, the interplay of inflammation, demyelination and neurodegeneration in the central nervous system alters the brain's functioning. Currently, little is known on how this complex interplay affects the activation and deactivation of large-scale, ongoing brain networks during rest.

One of the most commonly used techniques to examine the human brains functioning is functional magnetic resonance imaging (fMRI). FMRI allows assessing variations in blood oxygenation in different brain regions and is thus a proxy of metabolic need and brain

activity at each specific location. When acquired during rest, the statistical co-variations of these signals are referred to as resting-state functional connectivity. Several resting-state fMRI studies have observed connectivity changes in multiple sclerosis patients (Bonavita et al., 2011; Cruz-Gómez, Ventura-Campos, Belenguer, Avila, & Forn, 2013; Faivre et al., 2012; Hawellek, Hipp, Lewis, Corbetta, & Engel, 2011; Louapre et al., 2014; Zhou et al., 2014). Studies including multiple sclerosis patients at early disease stages (disease duration <3 yrs) typically report a higher connectivity in multiple sclerosis with positive correlations with cognitive impairment (Faivre et al., 2012; Hawellek et al., 2011; Zhou et al., 2014), whereas studies including more advanced multiple sclerosis patients typically report a lower connectivity and a negative correlation with cognitive abilities (Bonavita et al., 2011; Cruz-Gómez et al., 2013; Louapre et al., 2014). However, such fMRI studies have major limitations to examine the neuropathophysiology of multiple sclerosis. The intrinsic temporal smoothing induced by the slow haemodynamic response reduces our ability to assess the brain's fast dynamics. Furthermore, its indirect nature obfuscates the interpretation of the observed changes as they may be caused by modifications in metabolic consumption of a specific brain area or by alterations in the local neurovascular coupling between neuronal activity and haemodynamic status. This is especially relevant in multiple sclerosis in light of cerebral hypoperfusion (D'haeseleer et al., 2013; D'Haeseleer et al., 2015).

Electro- and magnetoencephalography (EEG/MEG) provide a more direct view on the brain's neuronal activity at the cost of a reduced spatial resolution. EEG/MEG studies have shown increases in power density in low frequencies (Leocani et al., 2000) and changes in alpha-band connectivity in multiple sclerosis patients (Tewarie et al., 2013). Yet, an important shortcoming of many neurophysiological studies in multiple sclerosis is the omission of treatment covariates. As such, discrepant research findings may be explained by different treatment strategies in different clinical centres. The most commonly administered symptomatic treatment is the administration of benzodiazepines (BZDs). This class of pharmaceutical products is often administered in multiple sclerosis patients to reduce insomnia, spasticity, or anxiety. Although benzodiazepines lead to an increase in beta-power through an increase in GABAergic conductance (Jensen et al., 2005), little is known about the temporal, spectral and spatial specificity of this increase. Given the widespread administration of BZDs in multiple sclerosis and their strong effect on neurophysiological functioning, BZD administration is the main confounder to be included.

Previous studies have focussed primarily on the spatial and frequency dimension of multiple sclerosis or BZD induced neurophysiological changes. In this study, we aim to deepen our understanding by incorporating the temporal dimension: instead of describing the brain's oscillations as sustained oscillations, we consider them as transient bursts in specific brain networks (van Ede, Quinn, Woolrich, & Nobre, 2018). For this, we apply a hidden Markov model (HMM) approach (Baker et al., 2014; Vidaurre et al., 2016; Vidaurre et al., 2018) which, in contrast to a microstate analysis (Gschwind et al., 2016) that only looks at instantaneous topographies and does not separate the temporal and frequency dimension, results in the identification of large-scale ongoing brain networks that are activated in bursts. The average duration of these bursts is referred to as the mean lifetime of a specific state and can be compared across subjects.

In this study, we investigated whether the brain's fast temporal dynamics are affected in multiple sclerosis patients and whether these changes are induced by the pathology or by the use of benzodiazepines (BZDs). Based on the EEG-microstate analysis by Gschwind et al., we expect increased lifetimes of the sensorimotor states (Gschwind et al., 2016) in the multiple sclerosis cohort. Furthermore, we expect BZDs to increase beta power only in sensorimotor brain states and alter the brain's preference of visiting these states. We demonstrate that both the pathology and a symptomatic treatment such as benzodiazepines affect the brain's dynamics.

2 | MATERIALS AND METHODS

2.1 | Participants

We collected magnetoencephalographic data (MEG) and T1-weighted magnetic resonance imaging in a cohort of 90 multiple sclerosis patients and 46 matched healthy controls (HCs). Patients with multiple sclerosis were recruited at the National MS Center Melsbroek (Belgium). Inclusion criteria were: diagnosis with relapsing remitting or progressive multiple sclerosis according to the revised McDonald criteria (Polman et al., 2011), age between 18 and 60 years old and having and an expanded disability status scale [EDSS, (Kurtzke, 1983)] < = 6. Exclusion criteria were a relapse or treatment with corticosteroids in the 6 weeks preceding the study, pacemaker, dental wires and concomitant psychiatric disorders (e.g., major depressive disorder) and epilepsy.

2.2 | Ethics

All subjects provided written informed consent and the study was approved by the local ethics committees of the University Hospital Brussels (Commissie Medische Ethiek UZ Brussel, B.U.N. 143201423263, 2015/11) and the National MS Center Melsbroek (February 12, 2015).

2.3 | MEG and MRI data collection

The MEG data were collected at the ULB Hôpital Erasme (Brussels, Belgium) on an Elekta Neuromag Vectorview scanner for the first 30 multiple sclerosis patients and 15 HCs and on an Elekta Neuromag Triux scanner for the remaining cohort due to an upgrade. Both MEG scanners share similar sensor layout (102 triple sensors, each consisting of one magnetometer and two orthogonal planar gradiometers) and were placed in a lightweight magnetically shielded room (Elekta Neuromag & Maxshield™, Elekta Oy, Helsinki, Finland). As changes with respect to signal-to-noise-ratio or sensitivity to specific frequency bands may affect results, we included the MEG scanner type as a covariate in our statistical models (cf. Statistics).

During MEG data collection, all participants were asked to close their eyes and think of nothing specifically (eyes-closed resting-state

condition) for 10 min. All subjects were continuously monitored not to fall asleep.

MEG signals were recorded at 1 kHz sampling rate with a 0.1–330 Hz pass-band filter. Subjects' head position inside the MEG helmet was continuously monitored using four head-tracking coils. The location of these coils and at least 400 head-surface points (on the nose, face and scalp) with respect to anatomical fiducials were determined with an electromagnetic tracker (Fastrak, Polhemus, Colchester, Vermont). The subjects' head movement was assessed using continuously energised head position indicator coils.

Simultaneous with the MEG signal acquisition, electrooculogram (EOG) was recorded using four EOG electrodes to capture horizontal and vertical eye movements and electrocardiogram (ECG) was measured using two electrodes on the participants' wrists.

Magnetic resonance imaging (MRI) was performed on a 3 T Achieva scanner (Philips Medical Systems, Best, The Netherlands). The scanner protocol contained a 3D T1-weighted sequence with parameters: TR: 4.939 ms, FA 8°, 230 × 230 mm^2 FOV, 310 sagittal slices; resulting in a 0.53 by 0.53 by 0.5 mm^3 resolution. This image was affinely coregistered to the MNI152 atlas.

The median delay between the MRI and MEG session across all subjects was 5 days with an interquartile range of 2–10 days. The maximal delay between MEG and MRI acquisition was 23 days.

2.4 | MEG preprocessing

MEG data were first preprocessed offline with the temporal extension of the signal space separation algorithm (Maxfilter™, Elekta Oy, Helsinki, Finland, version 2.2 with default parameters) to subtract external interferences and corrected for head movements (Taulu, Simola, & Kajola, 2005). Movement parameters were stored for later analysis.

All data were then downsampled to 250 Hz using an anti-aliasing filter, automatically coregistered with the subject's T1 image using RHINO, OSL's (https://github.com/OHBA-analysis) algorithm to coregister headshape points to the scalp extracted using FSL's BETSURF and FLIRT (Jenkinson, Pechaud, & Smith, 2002; Smith, 2002), and transformed in a common MNI152-space (Mazziotta, Toga, Evans, Fox, & Lancaster, 1995). Data were filtered between 1–70 Hz with an additional notch filter (48–52 Hz) using Butterworth filters of order removing line noise. After a visual check to remove artefactual time segments, an independent component analysis (ICA) was run to exclude ocular and cardiac artefacts based on the correlation of the ICA time courses with the electrooculograms and electrocardiogram and their spatial maps. After filtering into the frequency band of interest (1–40 Hz), source reconstruction was performed using a LCMV beamformer to an 8 mm cortical grid using a local sphere head model generated through FieldTrip as part of the standard OSL preprocessing pipeline (Oostenveld, Fries, Maris, & Schoffelen, 2011; Quinn et al., 2018; Woolrich, Hunt, Groves, & Barnes, 2011).

2.5 | Parcellation and orthogonalisation

The brain was parcellated using a custom parcellation atlas (42 parcels). Thirty-eight parcels were based on an ICA of fMRI data from the Human Connectome Project, the other four parcels correspond to the anterior and posterior precuneus and left and right intraparietal sulci as used before (Vidaurre et al., 2018). The parcellation atlas spanned the complete cortex and did not include subcortical areas. For each parcel, the first principal component of the time series within that parcel was used as that parcel's time series. All time series were orthogonalised using the symmetric multivariate leakage correction outlined in (Colclough, Brookes, Smith, & Woolrich, 2015) to ameliorate the effects of artefactual correlations induced by the ill-posed inverse problem.

2.6 | Static frequency content

The static frequency content was calculated using a multitaper approach based on Slepian functions with parameters set to provide a frequency resolution of 0.4 Hz. See Vidaurre et al. (2016) and Mitra & Bokil (2007) for more details. Where appropriate, we divided the spectrum into the traditional frequency bands: delta: 1–4 Hz, theta: 4–8 Hz, alpha: 8–12 Hz and beta: 12–30 Hz. Before entering statistical analyses, spectra were log10 transformed.

2.7 | Sign flipping

As the signs of source reconstructed time courses are arbitrary, data from multiple subjects cannot simply be concatenated. In Fingelkurts et al. (2004), this problem was addressed by applying a search approach to adjust the sign of the source-reconstructed time courses on the assumption that the covariance matrix between each pair of brain areas has the same sign across subjects. This algorithm flips the sign of the time series for some subjects and parcels in order to maximise the 'sign agreement' across covariance matrices. A more detailed mathematical description can be found in (Vidaurre et al., 2018). Source code and a more extensive description can be found on https://github.com/OHBA-analysis/HMM-MAR.

2.8 | The time-delay embedded hidden Markov model

When the data have been sign-flipped, it can be concatenated across all subjects and entered into the time-delay embedded hidden markov model (TDE-HMM) (Vidaurre et al., 2016; Vidaurre et al., 2018). This model has two important characteristics. First, it is Markovian and, as such, the probability of observing a specific state at time point T only depends on the state of time point T-1 and the data at timepoint T. Second, each HMM state is characterised by an observation model that describes the probability distribution of the data for that state. This observation model could be a multivariate autoregressive (MAR) model, which models the activity at timepoint T as a linear combination of the activation at a number of predefined previous timepoints. Yet, the large number of parameters involved makes this approach

cumbersome for whole-brain data. On these grounds, Vidaurre et al. proposed the TDE-HMM approach, which can be considered a simplification of the HMM-MAR model. In the TDE-HMM approach, lagged versions of the data are added to the original data, resulting for each subject in an extended data matrix of (Nchannels*Nlags) x Ntimepoints. Next, a principal component analysis is run to reduce the dimensionality by only including a predefined number of PCs, reducing the datamatrix to Npcs X Ntimepoints, with Npcs << Nchannels*Nlags. Finally, a standard Gaussian observation models is applied as described previously (Baker et al., 2014). We used the same parametrisation as in Vidaurre et al. 2018, with time lags varying between −7 and 7 timeframes, corresponding to windows of 60 ms and the number of PCs (84) chosen to be twice the number of actual sources (42).

Importantly, there is a trade-off between the number of PCs and the number of time lags taken into account. More lags and fewer PCs will render the model more sensitive to lower frequencies, whereas the opposite will render the model more sensitive to faster frequencies. Details about why short-lived states (e.g., below 200 ms) can capture theta and delta waves, which cycle at frequencies between 1 and 8 Hz and, thus, a period between 167 and 1,000 ms, can be found in Vidaurre et al. 2018. The TDE-HMM is run on the concatenated, normalised and sign-flipped data.

2.9 | Temporal characteristics

Once the HMM had run, we obtained for each timepoint and each state a probability that that specific state was active (referred to as 'HMM-Gamma'). Next, the Viterbi algorithm (Rabiner, 1989) was used to categorically designate each timeframe to a specific state. This was used to look at the temporal dynamics of each state: the fractional occupancy (FO, the proportion of time spent in that state), the frequency with which a specific state is active (Frequency of Occurrence, FreqOcc), the mean lifetime of each state (MLT), the mean interval (Int) between two consecutive occurrences of a specific state and the transition probabilities, that is, how often one state switches to another. Together, these quantities offer a summary of the brain dynamics as captured by the HMM (Baker et al., 2014). By splitting the HMM output per subject, we calculate these parameters for each subject individually.

2.10 | Spatial layout

We calculated each HMM state's spatial map as the correlation between that HMM state's time course and the parcels' time courses. This resulted in a spatial map for each subject and each state. The spatial configuration depicted in this paper displays the average across all subjects.

2.11 | State-specific spectral content

For each state and for each brain region, we define the state-specific time course as the multiplication of that brain region's time course with the probability that that state was active. The subject-, state- and brain region specific spectral power can then be calculating between 1 and 40 Hz applying a multi-taper approach in the same way as we did for the static analysis (Vidaurre et al., 2016).

2.12 | Benzodiazepines

The following benzodiazepines (BZDs) were identified within the multiple sclerosis cohort: Alprazolam, Clonazepam, Flurazepam, Lorazepam and Triazolam. The multiple sclerosis cohort was divided into two subcohorts: MS(BZD+) and MS(BZD−) depending on whether the patient received BZDs or not.

2.13 | Statistics

The static power and the HMM states' temporal characteristics, spectral content and spatial maps were compared between cohorts [HC vs. MS, MS(BZD+) vs. MS(BZD−)] after linear correction for scanner-version, age and education. In addition, when comparing the MS(BZD+) to the MS(BZD−) cohort, EDSS was also included as a covariate. As male subjects were only included when the study could be extended (after the scanner upgrade), gender and scanner type are correlated. Where necessary, the analyses have been repeated including only female or male participants.

A null-distribution of parametric t-statistics was generated using 1E4 random permutations of the cohort assignment. The *p*-value was calculated as the fraction of permutations with values more extreme than the observed statistic.

Correction for multiple comparisons was performed by considering the maximal value obtained across the considered parameters for each permutation and testing the observation against this distribution of maximum statistics. This procedure allows controlling the family wise error rate (Nichols & Hayasaka, 2003).

3 | RESULTS

After the description of the included cohort of multiple sclerosis patients and controls, we will first show the results of a standard static analysis displaying the effect of pathology and BZD treatment in distinct networks. Next, we will demonstrate the results of the dynamic analyses: we will compare the temporal dynamics and power spectrum between MS and HCs and between MS patients treated with BZDs and MS patients not treated with BZDs.

3.1 | Subject cohort

We included 90 multiple sclerosis patients with a mean age of 48.2 ± 9.9 years and 46 HCs with a mean age of 47.8 ± 12 years. Of these 90 multiple sclerosis patients, 22 were on BZDs at the time of the MEG session. Gender and EDSS differed significantly between the MS(BZD+) and the MS(BZD–) cohort, see Table 1. For all subjects, 8-min of artefact free data were available. Of 90 multiple sclerosis patients, 7 presented with a progressive onset and none of these

7 received specific drugs for the progressive course at the time of assessment. Only six patients received pain medication, five patients received tramadol, one Sativex.

3.2 | Use of benzodiazepines

Of the 22 subjects who were administered a benzodiazepine, 5 were on Alprazolam, 13 on Clonazepam, 2 on Flurazepam, 4 on Lormetazepam and 3 on Triazolam. Only four subjects were on a combination of different benzodiazepines: one combined clonazepam, lormetazepam and alprazolam, one Clonazepam with Lormetazepam, one Clonazepam with Flurazepam and one Alprazolam with Triazolam.

3.3 | Comparison of static frequency power

Comparing the complete multiple sclerosis cohort with the complete HC cohort did not reveal any significant difference in power. However, splitting the analysis according to gender revealed significantly lower power in the delta-band (1–4 Hz) in female multiple sclerosis patients (N = 42) as compared to female HCs (N = 27), cf. Figure 1a. In Figure 1b, we show that similar results are obtained when limiting the female multiple sclerosis cohort to the female multiple sclerosis cohort not treated by BZDs. Comparing male multiple sclerosis patients (N = 26) with male HCs (N = 19) revealed no differences in power.

3.4 | Benzodiazepines induce frequency content changes

By comparing the MS(BZD+) to the MS(BZD-) cohort, we identified an increased power in the beta-frequency (12–30 Hz) range in de MS(BZD+) group and a decreased power in the theta (4–8 Hz) range in the MS(BZD–) group, see Figure 2. The main differences were located in the sensorimotor area and the DMN.

Using NeuroSynth (neurosynth.org) to decode the images, the central sensorimotor area corresponds more specifically with the part related to the foot (correlation: 0.657). The correlation between the remaining activations and the DMN is 0.22.

3.5 | Comparison of transient dynamics

Whereas the static analysis assumes oscillations to be stationary, the TDE-HMM approach allows us to assess the temporal dynamics of transient bursts of oscillations and compare the temporal and spectral profiles for each brain state independently.

3.6 | Spatial maps of the transient states

Figure 3 presents the spatial maps associated with each of the 16 HMM states. Visual inspection shows networks similar to those in Vidaurre et al 2018, e.g., activation/deactivation of the occipital/visual network (states 8 and 11), sensorimotor network (states 2, 7, 9 and 12) and frontal (state 3) and posterior DMN (state 6). All states were present in all subjects as discussed in the supplementary material.

3.7 | Temporal properties of the transient states

The temporal dynamics of the transient brain states are summarised in four parameters (mean lifetime, fractional occupancy, frequency of occurrence and mean interval). Figure 4 shows the comparison of these novel features with respect to MS versus HC and benzodiazepine status after correction for education, scanner type and age.

3.8 | Correction for covariates

As discussed in the Methods, education, scanner type and age were all included as covariates. Across the whole group of 136 subjects, education did not correlate with any feature, age affected the frequency of occurrence of state 15 only (Pearson correlation, p = .01, uncorrected) and the scanner type affected state 6 (Pearson correlation, p = .002,

TABLE 1 Clinical characteristics

	HC	MS(BZD+)	MS(BZD-)	P(ANOVA)	P(BZD)
N	46	22	68	–	
Age (years)	47.8 (12)	47.8 (8)	48.3 (10)	0.95	0.70
Education (years)	15 (2)	13.4 (2)	14.1 (3)	0.01	0.42
Gender (M/F)	19/27	1/21	26/42	–	0.003
Disease duration (years)	–	14.3 (6.7)	16.8 (10)	–	0.29
EDSS	–	3.25 [2.5–4.5]	2.5 [2.0–4.0]	–	0.03
25FWT (s)	–	6.2 (1.8)	5.5 (2.3)	–	0.22
9HPT (s)	19.6 (2.2)	23.2 (5.7)	23.2 (8.5)	0.01	0.98
BZD duration (years)	–	3.5 [1–4]	–	–	–

Note: P(ANOVA) denotes the p-value of an unbalanced two-way ANOVA with Group as factor with levels "HC","MS(BZD+)" and "MS(BZD-)". The p-value P(BZD) assesses the comparison between the MS(BZD+) and MS(BZD-) cohorts using a Wilcoxon rank-sum test, except for gender where a Pearson's chi-squared test was used. BZD duration refers to the duration of the respective BZD treatment. Age, education and disease duration are expressed in years and (X) refers to the *SD*. For EDSS and BZD duration, the values between square brackets denote the interquartile range.

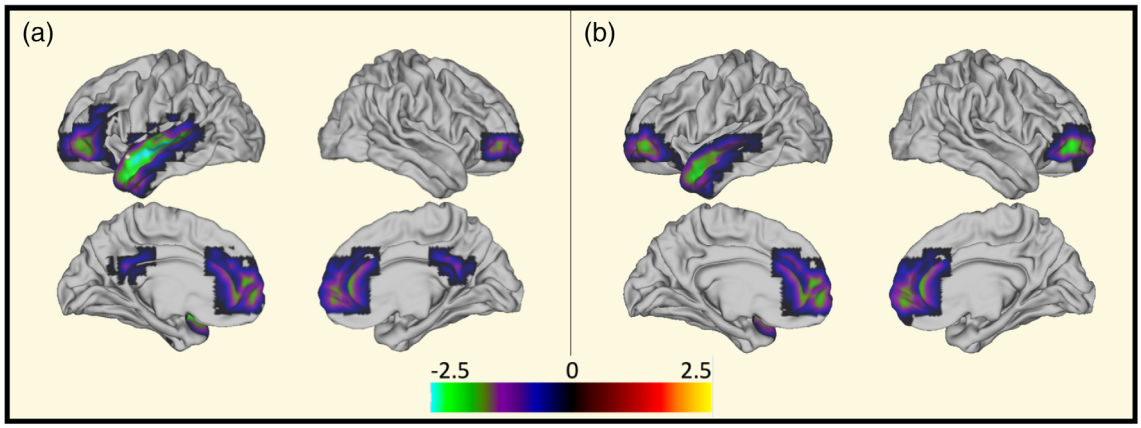

FIGURE 1 Reduced delta (1–4 Hz) power in female MS patients. Left: Reduced delta power in female MS patients as compared to female HCs. Right: Reduced delta power in female MS(BDP-) patients as compared to female HCs. The colour indicates-log10 (*p*-value). The *p*-values were generated using 10,000 permutations and were corrected for multiple comparisons across the 42 parcels, and only those *p*-values <.05 are shown. The negative sign denotes power losses in patients compared to HCs. MS, multiple sclerosis [Color figure can be viewed at wileyonlinelibrary.com]

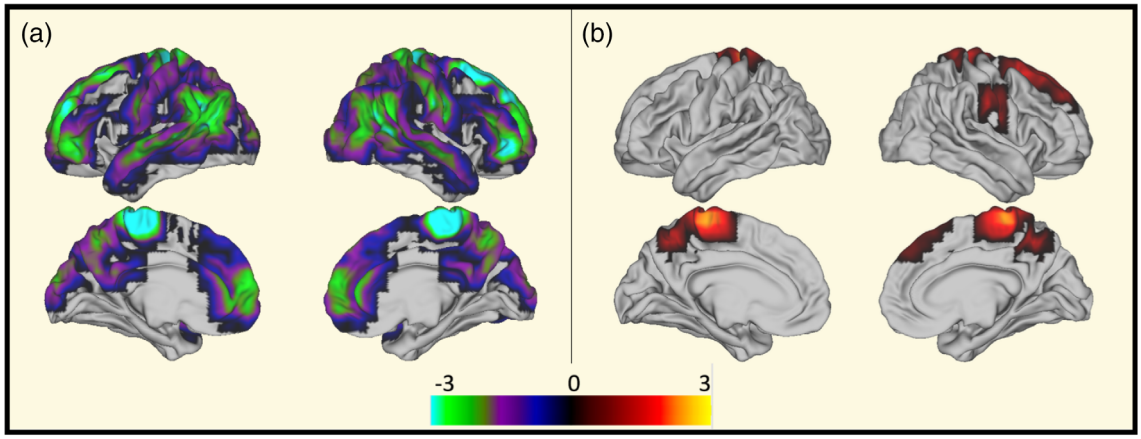

FIGURE 2 Increased beta (12–30 Hz) and reduced theta (4–8 Hz) power in MS(BZD+) versus MS(BZD–). Permutation-based *p*-values obtained after 10,000 permutations denoting differences in power between MS(BZD+) and MS(BZD–) patients in the different frequency bands (A: Theta, B: Beta). *p*-values are -log10 transformed and a positive sign indicates larger values in the MS(BZD+) cohort and negative values larger values in the MS(BZD–) cohort. Differences are primarily located in the sensorimotor network and the DMN. Only *p*-values <.05 after correction for multiple comparison across the 42 parcels are shown. Of notice, in a post hoc comparison within the identified 15–25 Hz band affected by BZDs, the ACC also shows a significantly increased beta power. MS, multiple sclerosis; BZD, benzodiazepine [Color figure can be viewed at wileyonlinelibrary.com]

uncorrected). However, when limiting the analyses to the MS and HC cohort respectively, no covariate contributed significantly.

3.9 | Multiple sclerosis versus healthy controls

We did not observe any significant difference when comparing the MS cohort to the HCs, nor when comparing the MS(BZD+) or MS(BZD–) sub cohorts with the HCs. Contrary to the static power analysis, no differences were disclosed when limiting the analysis to female subjects.

3.10 | MS(BZD+) versus MS(BZD–)

Figure 4 shows the uncorrected results. We observed a higher frequency of occurrence and fractional occupancy and a decreased mean interval for state 5; a decreased mean lifetime, fractional occupancy and frequency of occurrence of state 8; a reduced lifetime for state 11, an increased fractional occupancy, frequency of occurrence and decreased mean interval for states 12 and 16.

Applying a correction for multiple comparisons across all measures (four parameters x 16 states) based on nonparametric maximum statistics, only the increased frequency of occurrence for states 12 and 16 and a shorter mean lifetime for state 1 survived at $p < .05$. Obviously, there are strong relationships between these four temporal parameters (see Figure S1) by construction. Correcting for the four comparisons, but not correcting for the number of states additionally resulted in a significantly larger fractional occupancy of state 16 and a significantly shorter mean interval for state 5.

3.11 | Effect of gender

As can be noticed from Table 1, the MS(BZD+) and MS(BZD–) cohort differed significantly with respect to gender distribution, meaning that

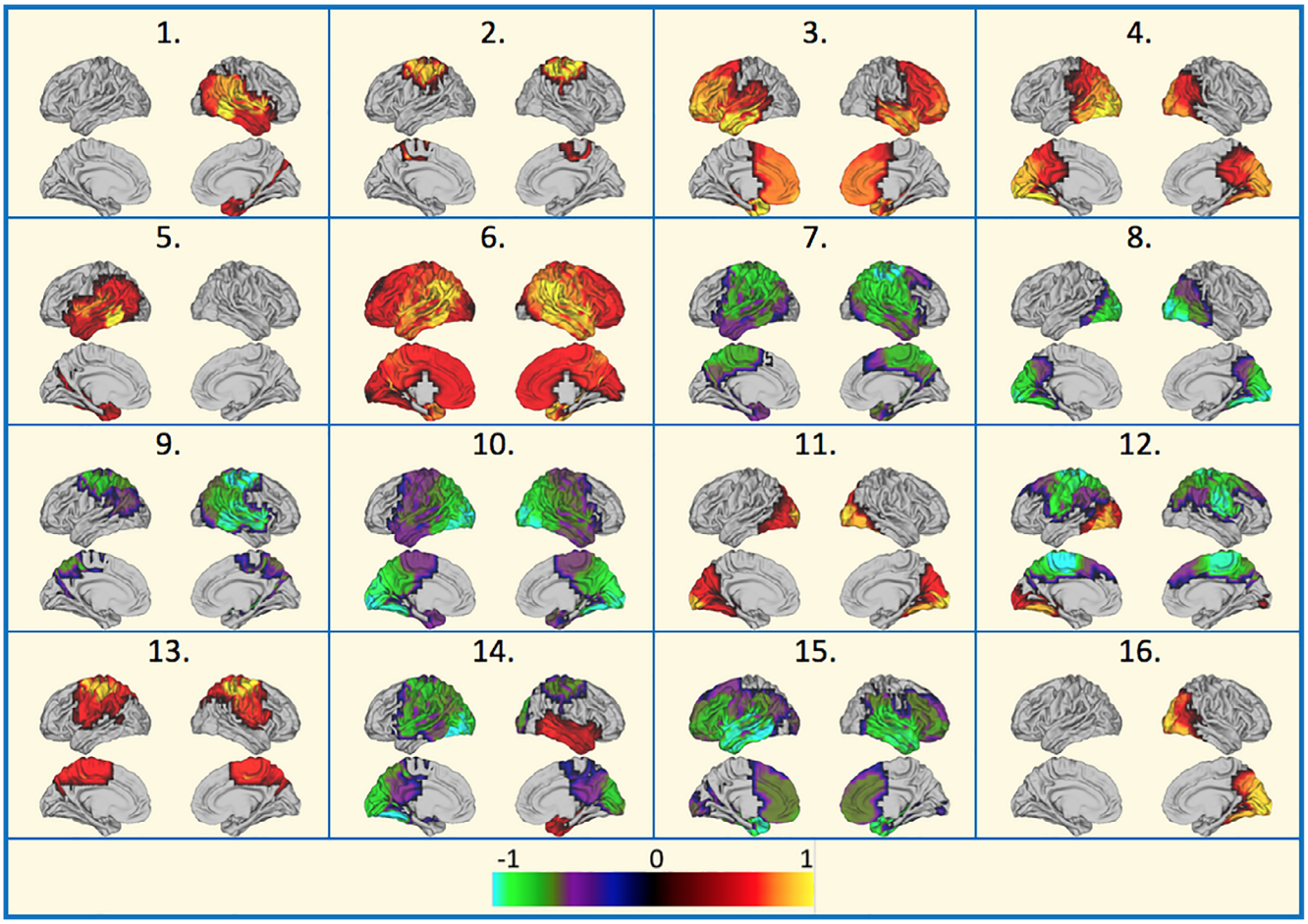

FIGURE 3 The spatial maps of the different HMM states. Each map represents the correlation between the HMM's state time course and the different parcels' activity. Maps are thresholded at 50% of their maximal value. HMM, hidden Markov model [Color figure can be viewed at wileyonlinelibrary.com]

the effect of gender and administration of benzodiazepines cannot be easily disentangled. Therefore, we included both gender and benzodiazepine-status in a two-factor ANOVA design as independent variables. This showed no significant effect of gender, whereas the significance of benzodiazepine was reduced but stronger than gender. Furthermore, we repeated the analysis including only female or male subjects with similar results.

3.12 | Comparison of the distribution of lifetimes

As summarising a single subject's distribution of lifetimes by the mean lifetime may not be the optimal choice, we compared—for each state—the distributions of lifetimes observed in healthy controls, MS(BZD–) and MS(BZD+) patients in a post hoc analysis using two-sample Kolmogorov–Smirnov tests.

Consistent with our previous results, the distribution of lifetimes of the MS(BZD-) cohort was shifted towards larger lifetimes (p: E-10) for state 8 (cf. Figure 4) as compared to the MS(BZD+) cohort. Additionally, the distribution of lifetimes for states 1, 11 and 15 were shifted towards larger lifetimes in the MS(BZD–) cohort with p-values of E-5.3, E-18 and E-5.8, respectively. Limiting the comparison to the largest female subcohort scanned on a single scanner, results in p-values of E-4.2, E-13 and 0.23, respectively. The distribution of lifetimes for state 9 was shifted towards larger lifetimes in the MS(BZD+) cohort with a p-value of E-10.

Despite the lack of significant differences in mean lifetimes when comparing the MS versus the HC, the distribution of lifetimes of state 15 was shifted towards larger lifetimes with a p-value of E-6.5. As this difference may be affected by the mixture of BZD+ and BZD– MS patients, we also compared the MS(BZD–) patients to HCs, resulting in a p-value of E-9.7.

Interestingly, analysing the results for male and female subjects separately, additional differences emerge. The distribution of lifetimes of male MS patients is significantly shifted towards larger lifetimes as compared with male healthy controls for states 3, 8 and 11 with p-values of E-28, E-6 and E-5.7, respectively. The opposite effect occurs when analysing female subjects with lifetime distributions shifted towards shorter lifetimes in female MS patients as compared to female healthy controls for the same states with p-values of E-7, E-5 and E-3.8.

3.13 | Comparison of transient frequency content

Whereas static power differences between the MS(BZD+) and the MS(BZD–) occurred in the theta and beta frequency bands (as shown in Figure 2), these differences were not captured equally by the

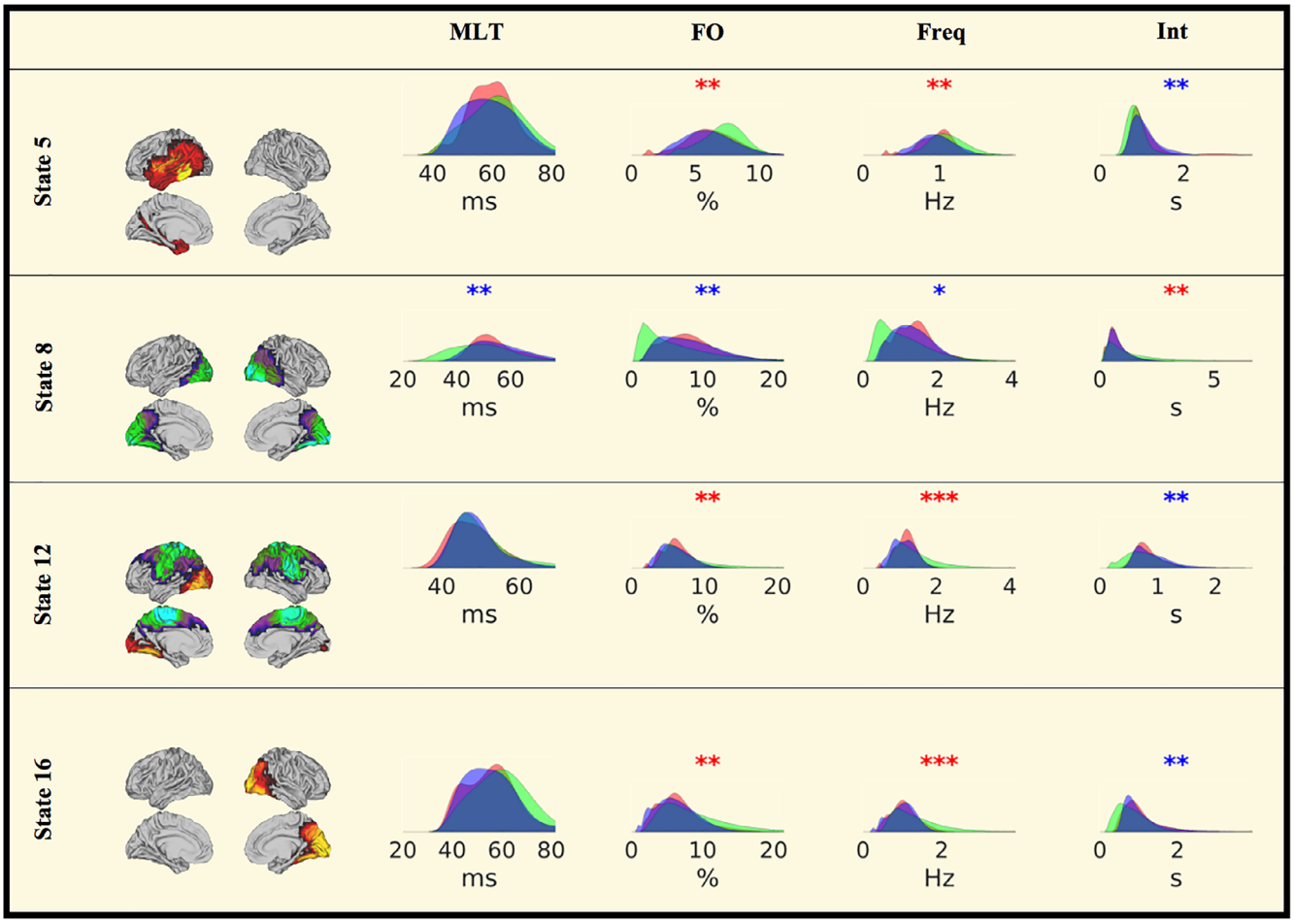

FIGURE 4 Temporal HMM characteristics. Red area: HC, blue area: MS(BZD−), green area: MS(BZD+). Red stars denote the significance of the permutation test MS(BZD+) > MS(BZD−) and blue stars of MS(BZD+) < MS(BZD−). No differences are observed between any of the two MS cohorts and the healthy control sample. *p < .05, **p < .01, ***p < .001 (uncorrected). MLT, mean lifetime; FO, fractional occupancy; Freq, frequency of occurrence; Int, mean interval between two consecutive occurrences. MS, multiple sclerosis; HMM, hidden Markov model; BZD, benzodiazepine [Color figure can be viewed at wileyonlinelibrary.com]

different HMM states. In Figure 5, we show for each HMM state (y = 1:16) and the static analysis (y = 17), the significance of the BZD-induced power differences. The HMM state (k = 6) with the highest power did not exhibit any BZD induced frequency power difference. Nor did the HMM states in which the sensorimotor network was active (states 2 and 13).

As the state-specific HMM frequency content was defined by applying the multitaper spectrum estimation to the timepoint-by-timepoint multiplication of the parcels' time courses and the probability of a specific state being active, their frequency content is the convolution of both frequency spectra. We provide a similar analysis focussing solely on the probability time courses only in Figure S1.

A similar analysis for the comparison of static and HMM-state specific power between female multiple sclerosis patients and female healthy controls resulted in the differences mainly being picked up by states 14 and 15, the deactivating occipital and temporal states. Yet, the differences were smaller and disappeared when averaged across all parcels.

4 | DISCUSSION

In this study, we demonstrated a reduced delta power in female multiple sclerosis patients as compared to female healthy controls and an increased beta power in multiple sclerosis patients treated with BZDs as compared to those not receiving BZDs. We found that this reduction in delta power in female multiple sclerosis patients was situated in the frontal DMN, whereas the increase in beta power and decrease in theta power observed in multiple sclerosis patients treated with BZDs affected both the sensorimotor network and DMN. Furthermore, leveraging the HMM approach, a novel analysis method capable of describing the brain's transient dynamics, we were able to show that BDZs induced an increase in beta power in all brain states, except for those that are associated with the activation of the sensorimotor network. Finally, we demonstrated how the distribution of lifetimes from MS patients differed significantly from HCs for different HMM states and that BDZs increased the FO and frequency of occurrence of the deactivating sensorimotor network.

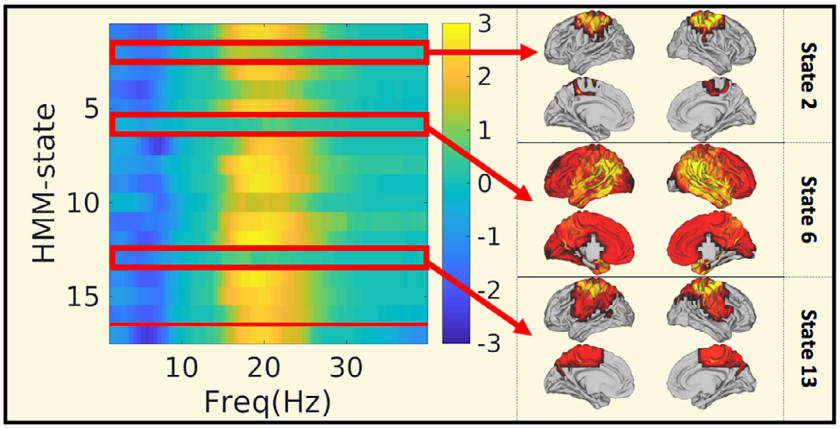

FIGURE 5 BZD induced changes in the static and HMM-specific frequency content. Comparison of static and HMM frequency content averaged across parcels between the MS(BZD+) and the MS(BZD−) cohort. The colour indicates -log10 of the *p*-value, with values ranging from 1.3 ($p = .05$) to 3 ($p = .001$). The sign of the *p*-value indicates the direction: Blue: Less power in MS(BZD+), yellow: More power in MS(BZD+). On the y-axis we have plotted the 16 HMM states and the static result (at y = 17). MS, multiple sclerosis; HMM, hidden Markov model; BZD, benzodiazepine [Color figure can be viewed at wileyonlinelibrary.com]

4.1 | Multiple sclerosis versus healthy controls

We first compared, for each parcel and frequency band (delta, theta, alpha and beta), the power between the multiple sclerosis cohort and the healthy controls and observed no significant differences in any frequency band. When limiting the analysis to female multiple sclerosis patients and female healthy controls, a decreased delta power was observed in the frontotemporal regions in the multiple sclerosis cohort. The delta-band is only rarely mentioned in previous studies, but in the same network, Leocani et al. observed an increase in EEG theta power (Leocani et al., 2000). The lack of difference when comparing the male cohort to male HCs may reflect the larger variability within the male cohort or may be due to the smaller sample size of male subjects in this study.

In contrast to Gschwind et al. (2016), we observed no significant differences in averaged temporal dynamics between healthy controls and multiple sclerosis patients. This lack of significantly different temporal dynamics between the MS-cohort and the HC cohort is surprising. Given the large number of multiple sclerosis patients and healthy controls, a lack of statistical power seems unlikely. Although the MS-cohort contained 83 relapsing onset and 7 progressive onset patients, which could introduce an increased variability within the multiple sclerosis group, none of the progressive onset patients were administered BZDs and repeating the analyses on the relapsing onset patients only did not alter our results. Yet, given the strong effect of BZDs, one could expect significant differences between the full MS and HC cohort when including more patients treated with BZDs.

An alternative explanation for this lack of significant difference in MS versus HC may lie in methodological issues. Recent research has shown that the HMM is biased towards fast-switching states, when the underlying ground-truth distribution of lifetimes is not geometric (Shappell, Caffo, Pekar, & Lindquist, 2019). As an extensive study on different HMM models is beyond the scope of the manuscript, we compared for each HMM state the distribution of lifetimes between the three different cohorts. As opposed to calculating the mean lifetimes per subject and state, this procedure does not summarise the distribution of lifetimes into one single metric.

Indeed, the distribution of lifetimes of the MS(BZD-) cohort was shifted towards larger lifetimes of state 15, a state that can be identified as the deactivating frontal DMN (cf. Figure 3). When further analysing these results for male and female subjects separately, we demonstrated larger lifetimes in male MS patients in the activating frontal DMN and activating and deactivating occipital states. These findings contrast with the female subcohorts where the opposite effect is shown (i.e., shorter lifetimes in female MS patients). These findings demonstrate a less dynamic frontal DMN in male MS patients, whereas the frontal DMN seems to be less activated in female MS patients. A dynamic DMN during cognitive tasks has been hypothesised to be important for normal cognitive functioning and the results obtained by (Eijlers, Wink, Meijer, & Douw, 2019) indicate that cognitively impaired MS patients demonstrate a reduced DMN flexibility.

These results not only indicate that summarising a subject's distribution of lifetimes by the mean lifetime is likely not the optimal choice, it also further corroborates the importance of gender-disease interactions in multiple sclerosis.

Although all patients have an EDSS below or equal to six, the included cohort does span a wide range of disease duration and age and, therefore, different disease stages. Focussing on female subcohorts with short (<10 years, $N = 19$) or large (>20 years, $N = 20$) disease duration did not reveal any differences with matched subcohorts of the HCs. Also, within the multiple sclerosis cohort, no correlations were observed with disease duration or the EDSS.

4.2 | Neurophysiological effects induced by benzodiazepines

With respect to the effect of BZDs, we observed a decrease in theta power and increase in beta power. The increase in beta-band power was mainly located between 15 and 25 Hz within the sensorimotor regions. Although very few literature is available on the effect of Clonazepam, the effect of other benzodiazepines on EEG power has been shown in the literature (Fingelkurts et al., 2004; Gongora et al., 2015; Kopp, Rudolph, Löw, & Tobler, 2004). Clorazepate was already investigated by Buchsbaum et al. who showed decreases in occipital alpha and parietal theta and increases in posterior alpha and parietal beta in healthy controls (Buchsbaum et al., 1985). More recently, diazepam was shown to decrease delta and theta and increase beta power in

rats during open field behaviour (Lier, Drinkenburg, Eeten, & Coenen, 2004). The networks affected by benzodiazepines were however unclear and difficult to investigate using low-density EEG.

The increase in beta power in the sensorimotor network aligns with (Jensen et al., 2005) who demonstrated beta enhancement within the motor cortex of healthy controls. Possibly, this strong effect may be explained by the larger density of the $GABA_A$ receptor in this network (La Fougère et al., 2011) which may strengthen the effect of BZD-induced increased GABA-mediated inhibition and hence the beta power (Jensen et al., 2005). However, as the sensorimotor cortex also produces the strongest beta power, the spatial distribution of the effect of benzodiazepines may simply follow the spatial distribution of the beta power.

Apart from the larger beta power in sensorimotor areas, a reduced theta power was observed in cortical regions typically associated with the DMN. Whereas this is the first study to demonstrate the modulation of theta power by BZDs in the DMN, this is not a surprising finding as BZDs typically induce a reduction of anxiety and the DMN connectivity has been demonstrated to be implied in anxiety and anxiety disorders (Broyd et al., 2009; Coutinho et al., 2016; Tao et al., 2015; Zhao et al., 2007). Our present results strongly suggest that the anxiolytic effects of benzodiazepines relate to pharmacological effects on GABA neurotransmission specifically within the DMN or between the DMN and other brain structures. Interestingly, the same high-resolution PET study as mentioned earlier, demonstrated an increased $GABA_A$ binding potential within the DMN (La Fougère et al., 2011). As with the effect on beta power, significant differences in theta power occur in those regions where theta is strongest and could therefore reflect the spatial distribution of theta rather than a spatial specificity of BZDs.

The TDE-HMM analyses demonstrated a significantly larger frequency of occurrence and fractional occupancy of the activating occipital and left-temporal state and deactivating sensorimotor state and a lower fractional occupancy of the deactivating occipital state in the cohort of multiple sclerosis patients treated with benzodiazepines. The increased fractional occupancy of the deactivating sensorimotor network could be interpreted as this network being less dominant, consistent with the aim of administering BZDs to reduce spasticity.

Despite our evidence on how BZDs affect brain functioning in multiple sclerosis patients, it remains to be investigated how BZDs affect brain functioning in healthy controls and whether the observed effects are specific to specific sub-classes of BZDs or are a more general characteristic of BZD use.

The EEG microstates with increased lifetimes were hypothesised by Gschwind et al. to correspond to a sensorimotor or auditory network and the visual system (Gschwind et al., 2016). This hypothesis partially fits with our findings: similar to Gschwind et al. we observe an increased fractional occupancy of the sensorimotor network; yet, we observe an increase of the fractional occupancy of the activating occipital network and a decrease of the deactivating occipital network. Additionally, we observe significant changes in an activating left temporal network.

4.3 | Transient frequency power

As the HMM approach extracts brain states that are temporally, spatially and frequency specific, we compared the frequency content of the different HMM states for the two main comparisons [MS vs. HC and MS(BZD+) vs. MS(BZD−)]. Similar as in the static analysis, we observed significant power differences in the theta and beta-bands with respect to the multiple sclerosis patients' benzodiazepine status. Interestingly, the larger beta-power in the sensorimotor region is mainly expressed in those brain states, not associated with the sensorimotor network.

4.4 | Correlation of static frequency power with temporal dynamics

Despite the finding that the increase in beta power seems to be present in almost all HMM states, it should be noted that strong correlations exist between the temporal properties of the HMM states and the static frequency content averaged across the considered frequency bands. This indicates that the administration of benzodiazepines not only entails an increased background beta power, but also simultaneously alters the brain's preference to visit specific brain states.

4.5 | Limitations

The most common indication for BZD administration was to alleviate insomnia (17/23). Given that resting-state paradigms may induce sleepiness, it could be hypothesised that multiple sclerosis patients treated with BZDs are more likely to fall asleep or become drowsy during the recording. Yet, in that case, one could expect the MS(BZD+) cohort to (a) have increased power in the theta-band (b) to report higher values of fatigue and (c) to have larger movements within the scanner. As theta-band activity was reduced and as we did not observe higher self-reported fatigue levels nor larger movements, we are confident that the reported effects are not caused by MS(BZD+) subjects being more likely to fall asleep.

Other indications included spasticity (4/23), fear and trigeminal neuralgia. The question can thus be raised whether any observed difference could be due to increased movement during the MEG scanning session. Yet, there were no significant differences in the average displacements between the different cohorts.

Next, it is important to note that although we included gender, scanner type and EDSS score as covariates in the different GLMs, we also redid the analyses the largest female subcohort scanned on one scanner. Whereas no result survived correction for multiple comparisons when comparing the averaged temporal dynamics between the MS(BZD−) cohort and the MS(BZD+) cohort, the effect sizes were strongly correlated with those observed in the original analyses ($r = 0.82$, $p < E\text{-}25$), suggesting a lack of statistical power in this subcohort because of the smaller sample size. Furthermore, limiting the analyses of the pooled distributions of lifetimes to specific subcohorts did not affect the results significantly either.

A final limitation relates to the time-delay embedded HMM method. This approach has previously been shown to be capable of

characterising relevant brain networks and dynamics (Vidaurre et al., 2018) while being computationally feasible. An important limitation of these models, however, is that they might sometimes induce certain propensity towards having too quick transitions. This could be solved by explicitly modelling each state's duration in a hidden semi-Markov model (HSMM) (Yu, 2010), which was previously applied on functional MRI data (Faisan, Thoraval, Armspach, & Heitz, 2003). In line with this argument, (Shappell et al., 2019) demonstrated that both HSMMs and HMMs perform equally well on the estimation of different states and the transition matrix, but that HSMMs outperform HMMs when estimating lifetimes that do not follow a geometric distribution. Future research should elucidate whether HSMM can provide more reliable estimates of lifetimes in MEG data as compared to the HMM.

5 | CONCLUSION

We demonstrated gender-dependent changes in the dynamics of the frontal DMN in multiple sclerosis patients. Furthermore, a symptomatic treatment such as benzodiazepines was shown to affect the brain's dynamic. Indeed, administration of benzodiazepines not only entails an increase in beta power, but also alters the brain's preference to visit specific brain states with an increased preference for the deactivating sensorimotor network consistent with the administration of BZDs with the aim of reducing spasticity. To the best of our knowledge, this study is the first to characterise the effect of multiple sclerosis and BZDs in vivo in a spatially, temporally and spectrally defined way.

ACKNOWLEDGMENTS

We would like to thanks all participants (healthy controls and people with multiple sclerosis) for their time and enthusiasm to participate, Ann Van Remoortel for her help in the recruitment and Jeroen Gielen and Jorne Laton for their help in the data collection.

CONFLICT OF INTERESTS

The authors report no competing interests.

ORCID

Jeroen Van Schependom https://orcid.org/0000-0003-1200-5872
Diego Vidaurre https://orcid.org/0000-0002-9650-2229
Lars Costers https://orcid.org/0000-0003-2668-8061
Marie B. D'hooghe https://orcid.org/0000-0002-0917-4176
Serge Goldman https://orcid.org/0000-0002-9917-8735

REFERENCES

Baker, A. P., Brookes, M. J., Rezek, I. A., Smith, S. M., Behrens, T., Probert Smith, P. J., & Woolrich, M. (2014). Fast transient networks in spontaneous human brain activity. *eLife*, *3*, e01867–e01867.

Bonavita, S., Gallo, A., Sacco, R., Corte, M. D., Bisecco, A., Docimo, R., … Tedeschi, G. (2011). Distributed changes in default-mode resting-state connectivity in multiple sclerosis. *Multiple Sclerosis Journal*, *17*, 411–422.

Broyd, S. J., Demanuele, C., Debener, S., Helps, S. K., James, C. J., & Sonuga-Barke, E. J. S. (2009). Default-mode brain dysfunction in mental disorders: A systematic review. *Neuroscience and Biobehavioral Reviews*, *33*, 279–296.

Buchsbaum, M. S., Hazlett, E., Sicotte, N., Stein, M., Wu, J., & Zetin, M. (1985). Topographic EEG changes with benzodiazepine administration in generalized anxiety disorder. *Biological Psychiatry*, *20*, 832–842.

Colclough, G. L., Brookes, M. J., Smith, S. M., & Woolrich, M. W. (2015). A symmetric multivariate leakage correction for MEG connectomes. *NeuroImage*, *117*, 439–448.

Coutinho, J. F., Fernandesl, S. V., Soares, J. M., Maia, L., Gonçalves, Ó. F., & Sampaio, A. (2016). Default mode network dissociation in depressive and anxiety states. *Brain Imaging and Behavior*, *10*, 147–157.

Cruz-Gómez, A. J., Ventura-Campos, N., Belenguer, A., Avila, C., & Forn, C. (2013). The link between resting-state functional connectivity and cognition in MS patients. *Multiple Sclerosis Journal*, *20*, 338–348.

D'haeseleer, M., Beelen, R., Fierens, Y., Cambron, M., Vanbinst, A.-M., Verborgh, C., … De Keyser, J. (2013). Cerebral hypoperfusion in multiple sclerosis is reversible and mediated by endothelin-1. *Proceedings of the National Academy of Sciences*, *110*, 5654–5658.

D'Haeseleer, M., Hostenbach, S., Peeters, I., El Sankari, S., Nagels, G., De Keyser, J., & D'Hooghe, M. B. (2015). Cerebral hypoperfusion: A new pathophysiologic concept in multiple sclerosis? *Journal of Cerebral Blood Flow and Metabolism*, *35*, 1406–1410.

Eijlers AJC, Wink AM, Meijer KA, Douw L (2019): Reduced Network Dynamics on Functional MRI Signals Cognitive Impairment in Multiple Sclerosis.

Faisan S, Thoraval L, Armspach J-P, Heitz F (2003): Hidden semi-Markov event sequence models: application to brain functional MRI sequence analysis:I-880-I–883.

Faivre, A., Rico, A., Zaaraoui, W., Crespy, L., Reuter, F., Wybrecht, D., … Audoin, B. (2012). Assessing brain connectivity at rest is clinically relevant in early multiple sclerosis. *Multiple Sclerosis Journal*, *18*, 1251–1258.

Fingelkurts, A. A., Fingelkurts, A. A., Kivisaari, R., Pekkonen, E., Ilmoniemi, R. J., & Kähkönen, S. (2004). The interplay of LORAZEPAM-induced BRAIN oscillations: Microstructural electromagnetic study. *Clinical Neurophysiology*, *115*, 674–690.

Gongora, M., Peressuti, C., Velasques, B., Bittencourt, J., Teixeira, S., Ariascarrión, O., … Ribeiro, P. (2015). Absolute Theta Power in the Frontal Cortex During a Visuomotor Task: The Effect of Bromazepam on Attention. *EEG and Clinical Neuroscience Society*, *46*(4), 292–298.

Gschwind, M., Hardmeier, M., Van De Ville, D., Tomescu, M. I., Penner, I. K., Naegelin, Y., … Seeck, M. (2016). Fluctuations of spontaneous EEG topographies predict disease state in relapsing-remitting multiple sclerosis. *NeuroImage: Clinical*, *12*, 466–477.

Hawellek, D. J., Hipp, J. F., Lewis, C. M., Corbetta, M., & Engel, A. K. (2011). Increased functional connectivity indicates the severity of cognitive impairment in multiple sclerosis. *PNAS*, *108*(47), 19066–19071.

Inglese, M. (2006). Multiple sclerosis : New insights and trends. *American Journal of Neuroradiology*, *27*, 954–957.

Jenkinson, M., Pechaud, M., & Smith, S. (2002). BET2-MR-based estimation of brain, skull and scalp surfaces. *Human Brain Mapping*, *17*, 143–155.

Jensen, O., Goel, P., Kopell, N., Pohja, M., Hari, R., & Ermentrout, B. (2005). On the human sensorimotor-cortex beta rhythm: Sources and modeling. *NeuroImage*, *26*, 347–355.

Kopp, C., Rudolph, U., Löw, K., & Tobler, I. (2004). Modulation of rhythmic brain activity by diazepam: GABA(a) receptor subtype and state specificity. *Proceedings of the National Academy of Sciences of the United States of America*, *101*, 3674–3679.

Kurtzke, J. F. (1983). Rating neurologic impairment in multiple sclerosis : An expanded disability status scale (EDSS). *Neurology*, *33*, 1444–1452.

La Fougère, C., Grant, S., Kostikov, A., Schirrmacher, R., Gravel, P., Schipper, H. M., … Thiel, A. (2011). Where in-vivo imaging meets

cytoarchitectonics: The relationship between cortical thickness and neuronal density measured with high-resolution [18F]flumazenil-PET. *NeuroImage*, *56*, 951–960.

Leocani, L., Locatelli, T., Martinelli, V., Rovaris, M., Falautano, M., Filippi, M., … Comi, G. (2000). Electroencephalographic coherence analysis in multiple sclerosis: Correlation with clinical, neuropsychological, and MRI findings. *Journal of Neurology, Neurosurgery, and Psychiatry*, *69*, 192–198.

Lier, H. V., Drinkenburg, W. H. I. M., Eeten, Y. J. W. V., & Coenen, A. M. L. (2004). Effects of diazepam and zolpidem on EEG beta frequencies are behavior-specific in rats. *Neuropharmacology*, *47*, 163–174.

Louapre, C., Perlbarg, V., Garc, D., Urbanski, M., Benali, H., Assouad, R., … Stankoff, B. (2014). Brain networks disconnection in early multiple sclerosis cognitive deficits : An Anatomofunctional study. *Human Brain Mapping*, *35*, 4706–4717.

Mazziotta, J. C., Toga, A. W., Evans, A., Fox, P., & Lancaster, J. (1995). A probabilistic atlas of the human brain: Theory and rationale for its development. The international consortium for brain mapping (ICBM). *NeuroImage*, *2*, 89–101.

Mitra, P., & Bokil, H. (2007). *Observed brain dynamics*. New York: Oxford University Press.

Nichols, T., & Hayasaka, S. (2003). Controlling the familywise error rate in functional neuroimaging: A comparative review. *Statistical Methods in Medical Research*, *12*, 419–446.

Oostenveld, R., Fries, P., Maris, E., & Schoffelen, J. M. (2011). FieldTrip: Open source software for advanced analysis of MEG, EEG, and invasive electrophysiological data. *Computational Intelligence and Neuroscience*, *2011*, 1–9.

Polman, C. H., Reingold, S. C., Banwell, B., Clanet, M., Cohen, J. a., Filippi, M., … Wolinsky, J. S. (2011). Diagnostic criteria for multiple sclerosis: 2010 revisions to the McDonald criteria. *Annals of Neurology*, *69*, 292–302.

Quinn, A. J., Vidaurre, D., Abeysuriya, R., Becker, R., Nobre, A. C., Woolrich, M. W., & Quinn, A. J. (2018). Task-evoked dynamic network analysis through hidden Markov modeling. *Frontiers in Neuroscience*, *12*, 1–17.

Rabiner, L. R. (1989). A tutorial on hidden Markov models and selected applications in speech recognition. *Proceedings of IEEE*, *77*, 257–286.

Shappell, H., Caffo, B. S., Pekar, J. J., & Lindquist, M. A. (2019). Improved state change estimation in dynamic functional connectivity using hidden semi-Markov models. *NeuroImage*, *191*, 243–257.

Smith, S. M. (2002). Fast robust automated brain extraction. *Human Brain Mapping*, *17*, 143–155.

Tao, Y., Liu, B., Zhang, X., Li, J., Qin, W., Yu, C., & Jiang, T. (2015). The structural connectivity pattern of the default mode network and its association with memory and anxiety. *Frontiers in Neuroanatomy*, *9*, 1–10.

Taulu, S., Simola, J., & Kajola, M. (2005). Applications of the signal space separation method. *IEEE Transactions on Signal Processing*, *53*, 3359–3372.

Tewarie, P., Hillebrand, a., Schoonheim, M. M., van Dijk, B. W., Geurts, J. J. G., Barkhof, F., … Stam, C. J. (2013). Functional brain network analysis using minimum spanning trees in multiple sclerosis: An MEG source-space study. *NeuroImage*, *88*, 308–318.

van Ede, F., Quinn, A. J., Woolrich, M. W., & Nobre, A. C. (2018). Neural oscillations: Sustained rhythms or transient burst-events? *Trends in Neurosciences*, *41*, 3–5.

Vidaurre, D., Hunt, L. T., Quinn, A. J., Hunt, B. A. E., Brookes, M. J., Nobre, A. C., & Woolrich, M. W. (2018). Spontaneous cortical activity transiently organises into frequency specific phase-coupling networks. *Nature Communications*, *9*, 2987.

Vidaurre, D., Quinn, A. J., Baker, A. P., Dupret, D., Tejero-Cantero, A., & Woolrich, M. W. (2016). Spectrally resolved fast transient brain states in electrophysiological data. *NeuroImage*, *126*, 81–95.

Woolrich, M., Hunt, L., Groves, A., & Barnes, G. (2011). MEG beamforming using Bayesian PCA for adaptive data covariance matrix regularization. *NeuroImage*, *57*, 1466–1479.

Yu, S. (2010). Hidden semi-Markov models. *Artificial Intelligence*, *174*, 215–243.

Zhao, X. H., Wang, P. J., Li, C. B., Hu, Z. H., Xi, Q., Wu, W. Y., & Tang, X. W. (2007). Altered default mode network activity in patient with anxiety disorders: An fMRI study. *European Journal of Radiology*, *63*, 373–378.

Zhou, F., Zhuang, Y., Gong, H., Wang, B., Wang, X., Chen, Q., … Wan, H. (2014). Altered inter-subregion connectivity of the default mode network in relapsing remitting multiple sclerosis: A functional and structural connectivity study. *PLoS ONE*, *9*, e101198.

SUPPORTING INFORMATION

Additional supporting information may be found online in the Supporting Information section at the end of this article.

How to cite this article: Van Schependom J, Vidaurre D, Costers L, et al. Altered transient brain dynamics in multiple sclerosis: Treatment or pathology? *Hum Brain Mapp*. 2019;40: 4789–4800. https://doi.org/10.1002/hbm.24737